The Water–Hydrophobic Interface: Neutral and Charged Solute Adsorption at Fluorocarbon and Hydrocarbon Self-Assembled Monolayers (SAMs)

Adam J. Hopkins,[a,†,*] Geraldine L. Richmond[a,b,*]

[a] *Department of Chemistry, University of Oregon, Eugene, OR 97403 USA*
[b] *Department of Chemistry, Materials Science Institute, University of Oregon, Eugene, OR 97403 USA*

Adsorption of small molecular solutes in an aqueous solution to a soft hydrophobic surface is a topic relevant to many fields. In biological and industrial systems, the interfacial environment is often complex, containing an array of salts and organic compounds in the solution phase. Additionally, the surface itself can have a complex structure that can interact in unpredictable ways with small solutes in its vicinity. In this work, we studied model adsorption processes on hydrocarbon and fluorocarbon self-assembled monolayers by using vibrational sum frequency spectroscopy, with methanol and butylammonium chloride as adsorbates. The results indicate that differences in surface functionality have a significant impact on the organization of adsorbed organic species at hydrophobic surfaces.

Index Headings: **Interface; Water; Methanol; Amine; Sum frequency; Surfactant.**

INTRODUCTION

Understanding molecular-scale interactions of adsorbates with fluorocarbon and hydrocarbon surfaces is of great importance for biological and industrial applications seeking to leverage the unique properties of fluorocarbons relative to their hydrocarbon counterparts. Biologically, fluorocarbon and hydrocarbon coatings are used for applications in drug-eluting stents and as coatings for hardening microelectronics against the harsh environment of the body.[1–5] Industrially, fluorocarbons and hydrocarbons are used in a wide array of wet- and dry-lubrication technologies.[6–8] In any of these systems, the coatings of interest are exposed to an array of chemical agents of varying functionality. Two of particular note are molecules with hydroxy and/or amine functionalities. Alcohols and similar small organic molecules are known to cause degradation of lubricant films in microelectromechanical applications.[7,8] Amines and amine chlorides are present in biological molecules and are commonly used in applications where cationic surfactants are required. In this study, we employed vibrational sum frequency spectroscopy (VSFS) to examine the adsorption of methanol and amines in aqueous solution to hydrocarbon (HC) and fluorocarbon (FC) surfaces. The studies were aimed at understanding the similarities and differences in how small polar and charged solutes interact with these two types of hydrophobic surfaces immersed in an aqueous solution.

Methanol (MeOH) is an ideal molecule to spectroscopically probe adsorption behavior on both FC and HC surfaces. First, the primary vibrational mode of the MeOH, which is the fundamental CH_3(ss) (symmetric stretching), occurs at 2830 cm^{-1} in the bulk liquid. This energy is approximately 40 cm^{-1} lower than a typical CH_3(ss). The frequency difference eases spectral analysis, because this mode does not overlap with vibrational modes of the HC and FC surfaces. Second, MeOH is electrically neutral. Previous reports showed that interfacial charge has a large effect on the VSFS spectra of interfacial water molecules at solid–liquid interfaces,[9–15] notably at both FC and HC surfaces,[10,16] due to differences in interfacial electrostatic fields. Adsorption of uncharged MeOH will be less affected by the interfacial electrostatic field than that of a charged species, which can be strongly enhanced or inhibited, depending on the sign of the charge. Finally, MeOH lacks a long carbon chain that causes self-ordering at the hydrophobic interface, as has been seen for dodecanol at octadecane thiol monolayers.[17] Freed from these strong interchain interactions that can drive adsorption, the degree to which lipophobicity versus hydrophobicity plays a role in adsorption at the FC surface can be more clearly determined.

Adsorption of a charged amine provides good contrast with the neutral MeOH. The majority of VSFS studies concerning charged species adsorption on hydrophobic surfaces has focused on relatively large molecules such as surfactants[18–24] and proteins[25–32] adsorbing at polymer surfaces. Long-chain alkylammonium salts are used in flotation of silica[33–38] and adsorption of long-chain amines has been studied by zeta potential,[33,37,38] infrared (IR) spectroscopy,[39–41] and VSFS.[42,43] These molecules exhibit complex aggregation and adsorption behavior because of van der Waals and/or electrostatic intermolecular interactions and, in the case of proteins, structural rearrangement as a function of pH and adsorbed state.[21,27,28,30,37] Small molecules simplify these difficulties, allowing investigation of the direct, molecular-level interactions between adsorbates and hydrophobic phases. Butylammonium chloride ($BuNH_3Cl$) has been chosen as a test molecule for this analysis for two principal reasons. First, this molecule exhibits properties between those of simple salts and neutral, polar organics. This salt is highly water soluble, and the carbon chain is not long enough to drive adsorption. However, at four carbons, it is sufficient to cause some molecular ordering.[41] Second, because the dissociation constant is very small, it has a nearly negligible effect on the solution pH and remains ionized even at low pH, meaning that the NH_2 species is not significantly present.

We previously conducted a comparative study of the structure of water at FC and HC self-assembled monolayers (SAMs) by using VSFS.[16] We found critical differences in the

Received 17 February 2012; accepted 19 September 2012.
* Authors to whom correspondence should be sent. E-mail: hopkins@alakai.us, richmond@uoregon.edu.
† Present address: Alakai Defense Systems, Largo, FL 33773, USA
DOI: 10.1366/12-06631

0003-7028/13/6703-0261/0

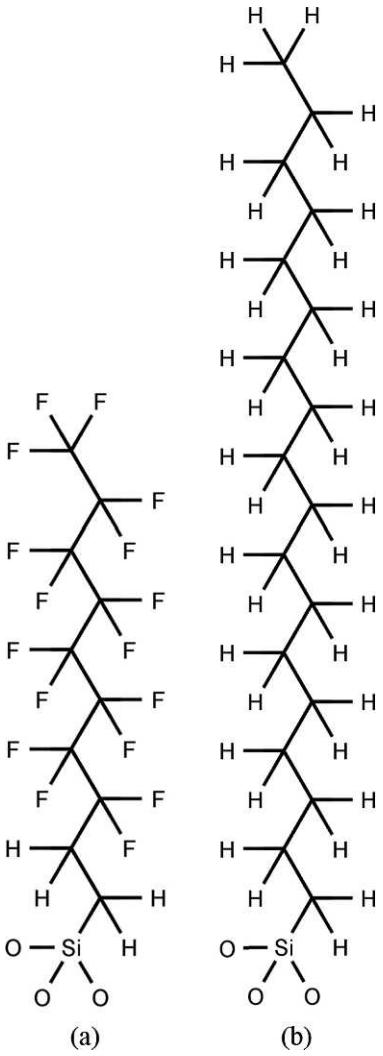

FIG. 1. Monomers used to make the SAMs described in this paper are (**a**) 1*H*,1*H*,2*H*,2*H*-perfluorodecylsilane (FDS) and (**b**) octadecylsilane (ODS).

molecular interaction between water and these two types of monolayers, most notably that water has more of a tendency to penetrate the HC coating, due in part to the slightly stronger interaction between water HC chains relative to FC chains. In this report, we show that differences in adsorption of two small organic molecules, MeOH and butylamine HCl ($BuNH_3Cl$), are driven by the unique interactions with both the FC and HC SAMs.

EXPERIMENTAL

VSFS was used in these studies to measure the vibrational spectrum of interfacial molecules. Over the past two decades, it has developed into a useful tool for characterizing, spectroscopically, a variety of complex interfaces.[17,21,45–49] VSFS response is generated by coupling two high-intensity laser sources in space and time at an interface between two immiscible phases. One of the laser sources is a fixed-frequency visible beam, and the other is a tunable IR beam. When the frequency of IR beam overlaps with that of a vibrational transition that is both IR and Raman active, a small amount of the incident light mixes and is coherently emitted at the sum of the incident frequencies. The principle advantage of VSFS is its ability to investigate buried interfaces without the production of large signal from the bulk media. By using the electric dipole approximation, this coherent emission is generated only by molecules in a noncentrosymmetric environment such as that at the solid–liquid interface. No contribution to the VSFS beam originates from molecules in the bulk liquid or solid environments; thus, the signal is limited to the few molecular layers experiencing net orientation at the interface. The frequency dependence of the VSFS response is unique to those molecules in the interfacial region, which allows for the characterization of interfacial structure and bonding. Furthermore, because VSFS is a coherent molecular process, the signal is polarization encoded and can be used to obtain molecular-orientation information. Within this report, three polarization combinations are used to better understand molecular orientation: SSP, SPS, and PPP; the letters denote the polarization of the sum frequency, visible beams, and IR beams, respectively. The SSP polarization exclusively probes components of the interfacial nonlinear susceptibility, $\chi^{(2)}$, containing information on the molecular transition dipole moment normal to the interfacial plane; SPS primarily probes the components parallel to the interfacial plane; and PPP polarized data contain all elements of the transition dipole moment. By comparing the vibrational modes in different polarization schemes, information about relative molecular orientation can be obtained. Extensive discussions of the principles and analysis of VSFS is found elsewhere in the literature.[50–55]

The VSFS system and sample setup used in this report were previously described.[16,56] In brief, a Spectra-Physics Lab 110 Nd:YAG, operating at 10 Hz, with a wavelength of 1064 nm, was used to pump an IR generation stage consisting of a potassium titanyl phosphate optical parametric oscillator coupled to a potassium titanyl arsenate optical parametric amplifier. The output of this stage ranges from 1 to 4 mJ across the usable wavelength range of 2600–4000 cm^{-1}, with a bandwidth of $\approx$2 cm^{-1}. The IR pulses are overlapped in space and time at the interface between the SAM and the liquid phase, with approximately 500 μJ of 532nm visible light generated by the frequency-doubled output of the master oscillator. The resulting VSFS photons are spatially and optically separated from the incident light before being collected by a photomultiplier tube. The raw VSFS spectrum is then normalized for variations in IR intensity and the absorption of IR by the silicone dioxide (SiO_2) prism and substrate. These processed spectra are then fit with an analytical global-fitting routine in IgorPro (Wavemetrics, Beaverton, OR), developed in our laboratory and modeled after the procedure introduced by Bain et al.[57,58] to attain more insight into the behavior of the systems investigated.

Hydrocarbon monolayers (octadecylsilane [ODS]) were prepared from octadecyltrichlorosilane (95%) and fluorocarbon SAMs were formed from 1*H*,1*H*,2*H*,2*H*-perfluorodecyltriethoxysilane (DFS; 95%) precursor molecules; the general form of these molecules is shown in Fig. 1. Both materials were purchased from Gelest (Tullytown, PA) and used after filtration through a 0.1 μm Teflon membrane to remove any large polymerization products and the copper stabilizer. The self-assembled monolayers of FDS and ODS were prepared with different methods due to differences in reactivity of the precusor molecules. We recently detailed the methods used.[16] FDS samples were deposited via the Langmuir–Blodgett

method at a surface pressure of 15 mN/m, with a maximum upward draw rate of 5 mm/min. Precursor molecules were spread on the surface of pH 2 HCl at a starting density of 1 molecule per 45Å^2 and equilibrated for 30 min to ensure that all the ethoxy groups were hydrolyzed. ODS samples were prepared from a dilute (2.3 mM) solution of octadecyltrichlorosilane in 4 : 1 (vol : vol) hexadecane–CCl_4 under near-anhydrous conditions. Samples were allowed to react for 6 h before being removed from the reaction matrix and rinsed copiously with hexadecane, acetone, and MeOH. All samples, ODS, and FDS, were cured at 110 °C for 1 h after initial formation and then stored in a vacuum desiccator cabinet until used.

Samples were initially characterized with atomic force microscopy (Nanoscope IIIa, Digital Instruments) and static water contact-angle measurements (KSV Theta). The samples were found uniformly hydrophobic by contact-angle measurement and free from large defects or silane aggregation products on the surface.

Three different MeOHs were used in the MeOH adsorption experiments: CH_3OH (Burdick and Jackson), CH_3OD (Sigma-Aldrich), and CD_3OD (Cambridge Isotopes). Solutions of CH_3OH–H_2O were used for VSFS studies including the O–H stretching region. CH_3OD–D_2O solutions were used for C–H stretching region experiments, because substituting OD for OH reduces the interferences with coordinated water-stretching vibrations. Both types of solutions were made by mass to account for changes in volume due to the mixing of the two liquids. The solution concentrations are measured in mole fraction (χ) of MeOH.

Several isotopomers of $BuNH_3Cl$ were used to study charged species adsorption. $BuNH_3Cl$ can be purchased from a number of suppliers; we found it in all cases contaminated with small amounts of other organic compounds, most likely butanol. As a result, we prepared the compound from liquid butylamine (Sigma-Aldrich) by reacting it stoichiometrically in a closed glass vessel, with slowly added concentrated hydrochloric acid. The reaction products were then dissolved in water to produce a ≈1 M solution. The solution pH was measured with a three-point calibrated pH meter and adjusted to the desired level by using small amounts of sodium hydroxide or HCl. This stock solution was then diluted to the desired amount by using pH 2 HCl or Nanopure water to make lower concentration solutions at pH 1.9 ± 0.1 and 5.7 ± 0.1. Deuterium-substituted butylammonium chloride salts were acquired from CDN Isotopes and used without further purification. Solutions of d_9–$BuNH_3Cl$ were prepared by dissolving the salt in aqueous pH 2 HCl and diluting to the desired concentration. $BuND_3Cl$ and d_9–$BuND_3Cl$ solutions were made by dissolving the molecules in pD 2 solutions of DCl (CDN Isotopes) dissolved in D_2O (Cambridge Isotopes).

RESULTS AND DISCUSSION

Methanol. Spectra of the neat FDS–H_2O and FDS–CH_3OH interfaces are shown in Fig. 2. The FDS monolayer is a coating of a 10-carbon-long molecule, as shown in Fig. 1a, with the top 8 carbons fluorinated and the bottom two serving as a hydrogenated spacer between the fluorocarbon and the silane group. The narrow feature in the FDS–H_2O spectrum near 2930 cm^{-1} is due to these CH_2 groups in the FDS monolayer. This feature is actually two distinct vibrational CH_2(as) (asymmetric stretching) modes at 2917 and 2954 cm^{-1}, as

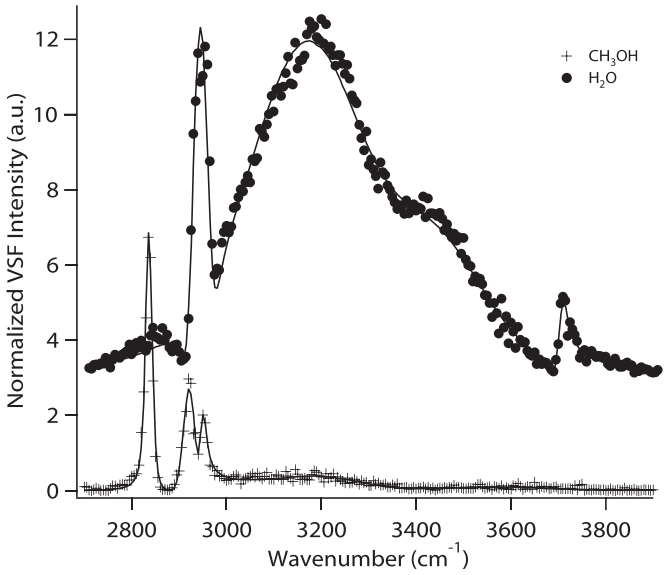

FIG. 2. VSFS spectra of the neat CH_3OH–FDS and H_2O–FDS interfaces.

determined by curve fitting. These modes are split due to the different bonding environments of the two CH_2 moieties; the latter is blue shifted from its native location by its bond with silicon. Shifts of similar magnitude were reported for methylsilane.[59] The broad features that dominate in the region from 3000 to 3600 cm^{-1} in this spectrum originate from water molecules with different degrees of coordination, from tetrahedrally bonded (lower-energy region) to progressively weaker bonding, up to 3600 cm^{-1}. The signal from water is enhanced due to the electrostatic field present at the surface and extending through the monolayer to orient the interfacial water. The electrostatic orientation arises primarily from penetration of water through defects in the SAM to the SiO_2 substrate, where it deprotonates nonbonded silanol groups, creating negative charge at the SiO_2 surface.[16] There is also a narrow mode in the FDS–H_2O spectrum at 3694 cm^{-1}, arising from the free-OH modes of the vibrationally decoupled OH oscillators of water molecules at the terminus of the FDS monolayer. For these water molecules, one OH bond is oriented toward the FDS surface (free OH), with which it weakly interacts, and the companion OH protrudes into the aqueous phase and is red shifted from the free OH due to its bonding interactions with other interfacial water molecules. Such sharp peaks were previously reported at the air–water[46,60], organic liquid–water,[61–64] and solid–water interfaces.[10,65,66] The frequency of this peak is a measure of the strength of the interaction between water and the hydrophobic phase.[16]

The FDS–CH_3OH spectrum in Fig. 2 appears to have three narrow peaks below 3000 cm^{-1}; however, careful analysis shows that there are actually five vibrational peaks present, which correspond to the two C–H stretching modes of the FDS monolayer and three CH peaks from CH_3OH. The methyl symmetric stretch of CH_3OH is spectrally distinct from the other CH vibrational modes of the SAM and is located near 2838 cm^{-1}. There is also a low, broad feature centered around 3050 cm^{-1}, which we attribute to the hydrogen bonding between CH_3OH molecules. From these OH modes and the lack of an uncoupled OH oscillator in the 3600 cm^{-1} region, it is clear that the CH_3 moiety, not the OH, is oriented toward the

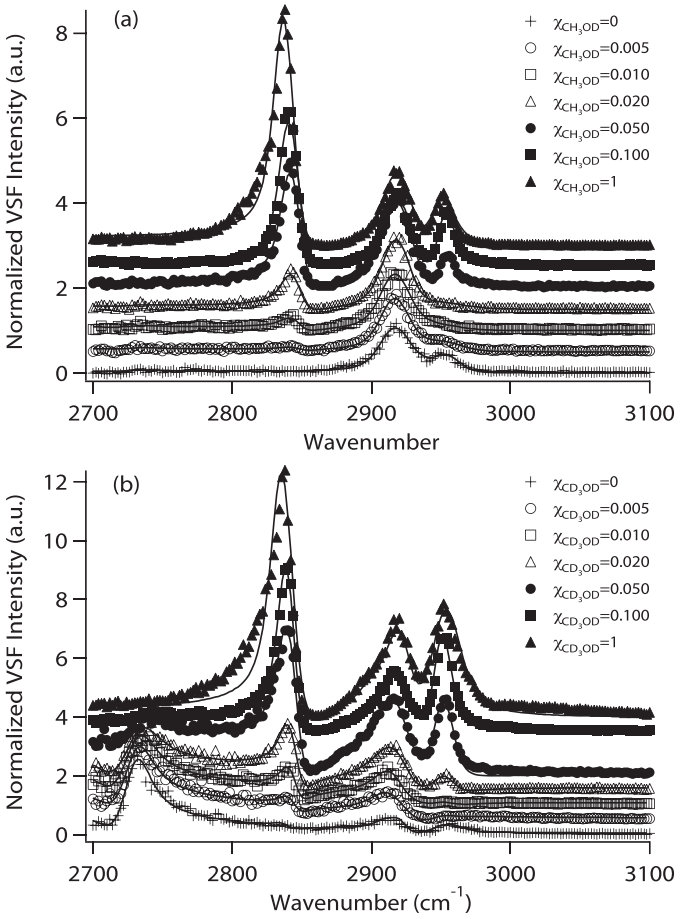

FIG. 3. (**a**) SSP- and (**b**) PPP-polarized VSFS spectra of CH_3OD:D_2O–FDS interface at several mole fractions of CH_3OD (χ). The spectra are fit to five resonances, three pure CH_3 peaks from CH_3OD and two CH_2 stretches from the monolayer. The spectra are offset for clarity.

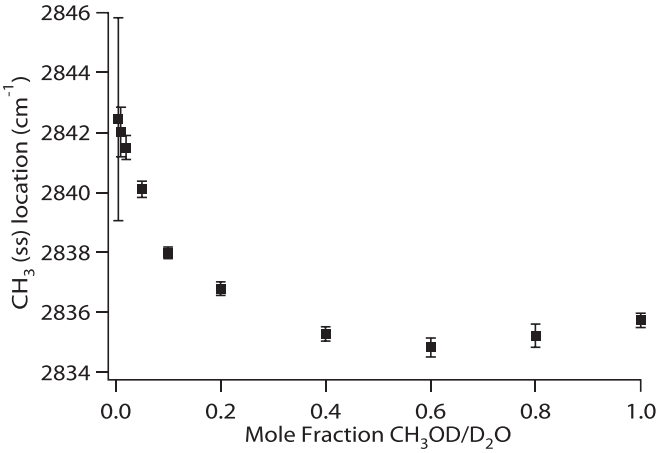

FIG. 4. Peak location of the CH_3(ss) at the FDS interface as a function of solution composition from spectral fitting.

monolayer. This is in agreement with previous observations of MeOH on octadecylsilane SAMs.[67]

Building on the above results, we examined how MeOH adsorption differs in the presence of water. To do this, the C–H stretching region was analyzed with solutions of partially deuterated MeOH, CH_3OD in D_2O. This shifted the broad resonance of the coordinated hydrogen bonding (seen in Fig. 2) out of the spectral window, largely freeing the data from this interference.

Selected VSFS spectra of the FDS–CH_3OD: D_2O system are shown in Fig. 3 in the SSP and PPP polarization schemes. The monolayer–D_2O spectrum, which is in the absence of CH_3OD, shows the distinct CH features of the FDS monolayer at 2917 and 2954 cm^{-1} in both polarizations. Adding a small amount of MeOH ($\chi = 0.005$) had almost no effect on the SSP spectrum in Fig. 3a, but increasing the concentration to $\chi = 0.010$ resulted in a small peak near 2840 cm^{-1} due to the MeOH. Increasing the concentration further increased the amplitude of this feature. The first CH_2(as) monolayer peak at 2917 cm^{-1} appeared to increase in strength with added MeOH. The second monolayer CH_2(as) peak at 2954 cm^{-1} seemed to decrease with the addition of CH_3OD through $\chi = 0.020$; after this, when the mole fraction was reached, the peak reappeared.

The PPP spectra in Fig. 3b have an additional peak that is not present in the SSP data from the free-OD vibrations near 2730 cm^{-1}. This peak is visible here because of the inclusion of vibrational modes from multiple elements of $\chi^{(2)}$. As CH_3OD was added to the interface, the amplitude of the free-OD peak decreased due to the displacement of the OD molecules. Otherwise, the PPP spectra followed the same trends as the SSP data.

The apparent complicated behavior of the monolayer stretching peaks observed in Fig. 3 is due to vibrational modes of MeOH overlapping with the monolayer CH modes. Spectral deconvolution can clarify this behavior. Liquid MeOH is known to have three peaks in the C–H stretching region near 2830, 2915, and 2940 cm^{-1} due to Fermi resonance interaction of the CH_3(ss) with two bending overtones;[68–70] our analysis found these peaks to be shifted by 5–15 cm^{-1} from these reported values. This shift is likely due to a combination of isotopic substitution and interfacial interaction effects. The primary peak with the most CH_3(ss) character is located at 2830 cm^{-1}, while the other two resonances are principally overtones that interfere with CH_2(as) stretches of the FDS monolayer and therefore require spectral fitting analysis for proper interpretation.

In a previous analysis, we determined that the CH_2(as) stretching vibrations from the FDS monolayer have opposite relative phases, to which we assigned values of 0 (2917 cm^{-1}) and π (2954 cm^{-1}).[16] Phases are determined from the spectral fitting analysis and indicate the relative orientation of the transition dipole moments in a spectrum. Meanwhile, the three MeOH modes all have relative phases of 0. As MeOH adsorbs to the interface, the higher-energy CH_3 Fermi resonance mode of CH_3OD, which we find occurs at 2953 cm^{-1}, interferes destructively with the 2954 cm^{-1} peak of FDS, causing the initial intensity decrease in this region of the low-concentration spectra in Fig. 3. As MeOH continues to accrue at the surface, the Fermi resonance of CH_3OD begins to dominate the FDS mode, which results in the reappearance of the peak near 2954 cm^{-1}. The other CH_3OD Fermi resonance peak is at 2923 cm^{-1} and has the same phase as the 2917 cm^{-1} mode from FDS. Thus, as the MeOH concentration is increased, the intensity in this region increases. The CH_3(ss) of CH_3OD is spectrally distinct and unambiguously grows in with increasing MeOH concentration.

Close examination of the spectra and the fitting results shows that the center frequency of the CH_3(ss) is not constant, but shifts to lower frequencies with increasing MeOH concentration until about 40 mole percent. Figure 4 shows this trend; the

error bars are the errors from the spectral deconvolution. Similar frequency shifts as MeOH concentration was increased were observed in bulk CH_3OH:H_2O solutions and at the solution–vapor and solution–ODS interface.[67,71–74] Density functional theory calculations suggest that when MeOH accepts hydrogen bonds, the CH_3(ss) vibrational frequency blue shifts by as much as 30 cm^{-1}.[71] Thus, changes in the hydrogen-bonding environment of interfacial MeOH can be used to explain the frequency shifting behavior. MeOH molecules are able to accept two hydrogen bonds and donate one. However, in pure MeOH, an interfacial molecule will on average accept only one hydrogen bond due to a lack of donor hydrogens. As the composition at the interface begins to include more water, each interfacial MeOH can accept more hydrogen bonds, because each H_2O molecule can donate two hydrogens. This increases the number of hydrogen bonds accepted by MeOH, which shifts the CH_3(ss) to a higher frequency, from 2837 to 2845 cm^{-1} in the case of the FDS interface.

With pure MeOH at the interface, the frequency of the CH_3(ss) is at 2837 cm^{-1}, not the 2830 cm^{-1} measured in liquid MeOH.[75–77] We attribute this frequency difference to the weaker interaction between the CH_3 moiety of MeOH and the fluorocarbon monolayer compared with MeOH–MeOH interactions. Additional support for this comes from the PPP spectra in Fig. 3b; the principle CH_3(ss) vibration of MeOH has the same relative phase as the free OD, which is known to protrude into the interfacial plane. The low-energy fluorocarbon–methyl group van der Waals interactions are weaker than those between methyl groups, which are the only neighbors in bulk MeOH. This interaction strength differential results in a blue shift of the CH_3(ss) frequency relative to bulk MeOH. In fact, the interfacial MeOH CH_3(ss) frequency at the FDS monolayer surface is the same as that measured for the MeOH–air interface,[73] where van der Waals interactions are also reduced relative to bulk CH_3OH.

To investigate orientational effects as CH_3OH adsorbs, the ratio of the fit amplitudes of the CH_3(ss) peak in PPP and SSP polarizations was examined. Figure 5a shows that this ratio is constant across the entire range of concentrations examined and indicates that MeOH adsorbs to the FDS interface with a constant orientation. Unlike long-chain alcohols or surfactants that change structure with solution concentration when adsorbing on hydrophobic solids,[17–19,78] the small MeOH molecules do not experience the strong interchain attractions that cause reorientation with changing concentration. Because the orientation of MeOH does not change with concentration, the number of MeOH molecules at the interface is directly proportional to the amplitude of the CH_3(ss) peak; thus, the amplitude is a measure of the effective surface number density.

This surface-adsorption isotherm is plotted in Fig. 5b. MeOH readily adsorbs to the surface of FDS, and the number density increases rapidly to a maximum near $\chi = 0.400$. The apparent surface number density decreases above this concentration. One possibility for this decrease is that as the concentration of MeOH exceeds 40 mole percent; MeOH absorbs in a second layer of opposite, albeit weaker, polar orientation, as has been suggested by Chen et al. In their analysis of the CH_3OH:H_2O–air interface.[74] For such a case, the VSFS signal from this second layer could partially cancel out the signal from the first layer, leading to a drop in the signal. This cancelation has been seen to occur at the interfaces

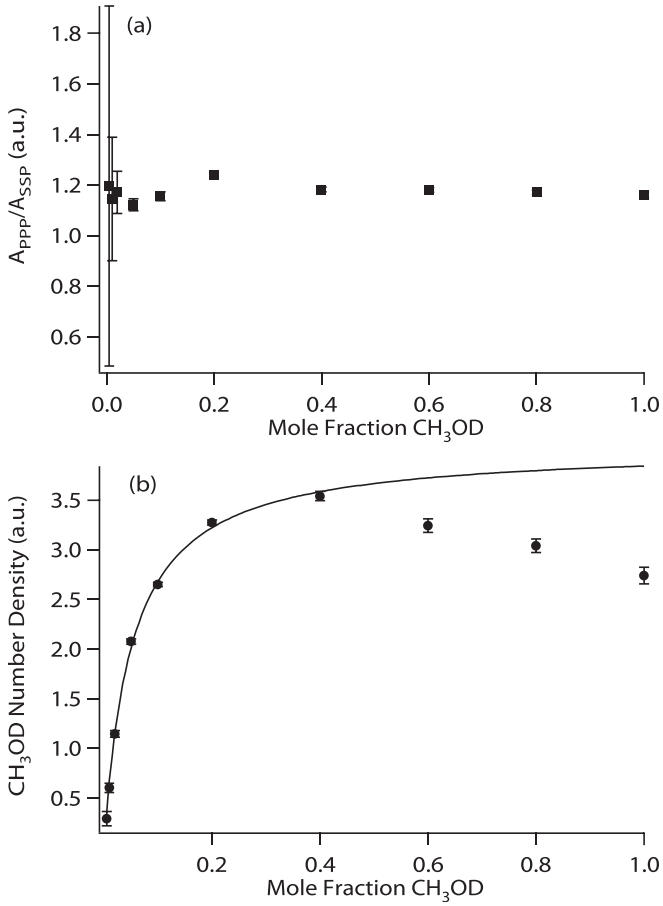

FIG. 5. (**a**) Fit amplitude ratio of the CH_3(ss) peak in the PPP (A_{PPP}) and SSP (A_{SSP}) polarizations at the FDS surface. (**b**) MeOH surface adsorption isotherm, from (A_{SSP}). The line is a fit to a standard Langmuir adsorption isotherm.

of several small alcohols with SiO_2.[44] A second possibility is that as the concentration of MeOH increases in the bulk, there is less driving force for CH_3OH to be at the interface and the actual MeOH number density decreases.

The results for MeOH at FC surfaces are different from what we measure at HC surfaces, where we found that the overall interaction strength of MeOH with FDS was lower than with ODS. This can be seen by both changes in the monolayer and the interfacial MeOH vibrational frequency. First, we compared the VSFS spectra of ODS with D_2O and CD_3OD; the resulting spectra are shown in Fig. 6. The D_2O–ODS spectrum shows two narrow peaks at 2874 ± 1 and 2938 ± 1 cm^{-1}, arising from the CH_3(ss) Fermi resonance pair of the chain terminus, as well as small contributions at 2912 ± 1 and 2960 ± 1 cm^{-1} due to the CH_2(as) of the alkyl chain and CH_3(as) vibrational modes, respectively. When the same ODS layer was exposed to CD_3OD, there was a small conformational change in the ODS layer, indicated by increased intensity near 2855 and 2912 cm^{-1}. This change indicates the formation of gauche defects in the monolayer,[79] brought about by the favorable attractive interaction between MeOH and ODS.

We employed the same strategy of using D_2O and CH_3OD to measure the spectra of ODS with MeOH (Fig. 7) so that the data would be free of interference from signals arising from O–H stretching modes. The addition of CH_3OD to the interface results in two obvious changes, (i) the appearance of a new peak below 2850 cm^{-1} and (ii) the disappearance of the ODS

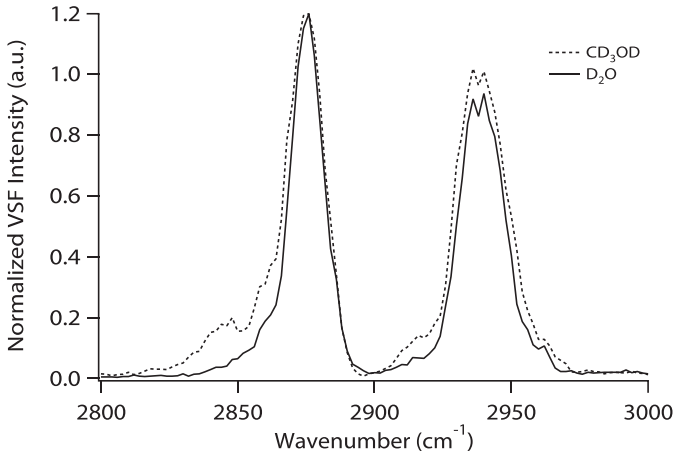

FIG. 6. VSFS spectra of an ODS–D_2O and ODS–CD_3OD interface. The spectra are scaled to the same value at 2874 cm^{-1}.

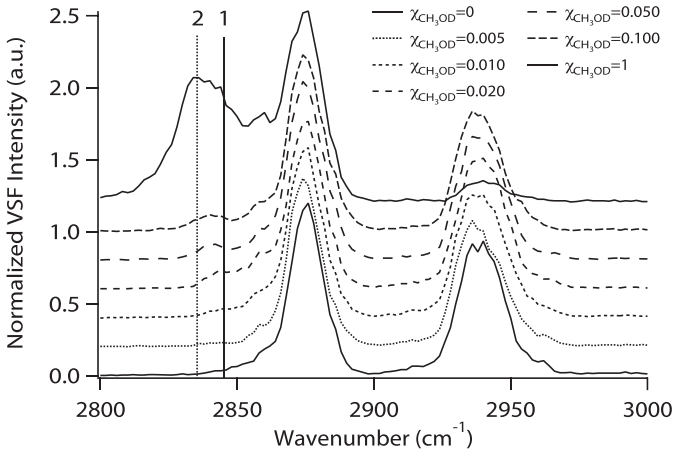

FIG. 7. SSP polarized VSF spectra of CH_3OD:D_2O–ODS interface at several mole fractions of CH_3OD (χ). The lines (***1***) and (***2***) indicate the CH_3OD peak location at $\chi = 0.1$ and $\chi = 1$, respectively. The spectra are offset for clarity.

mode near 2938 cm^{-1}. The signals arising near 2938 cm^{-1} decreased with the addition of CH_3OH, because the CH_3 Fermi resonances of MeOH were out of phase with the 2938 cm^{-1} peak of the ODS layer. The new peak arising in the spectra below 2850 cm^{-1} originated from the principle CH_3(ss) mode of MeOH, which has a bulk frequency of 2830 cm^{-1}. Due to the previously shown differences in the monolayer structure when the liquid phase is water or MeOH, a full spectral deconvolution of the data was not undertaken. Thus, we here limit analysis to two spectra for which the CH_3(ss) of MeOH is clearly visible, $\chi = 0.1$ and $\chi = 1$.

At $\chi = 0.1$ of MeOH, the MeOH peak has a frequency of 2838 $\pm$ 4 cm^{-1}; with pure MeOH on the surface, this frequency is shifted to 2831 $\pm$ 4 cm^{-1}. Though the uncertainties in the peak locations are larger than for FDS, the same trend of decreasing CH_3(ss) frequency with increasing MeOH concentration is present at both the ODS and FDS interfaces. Peak shifting of a similar magnitude was observed for this interfacial system by Liu et al.[67] However, the frequency of the CH_3(ss) vibration at ODS is several wavenumbers lower than at FDS. The lower frequency further shows that the molecular scale interactions between HC and HC are stronger than those between FC and HC. There is one other apparent similarity between the FDS and ODS systems. The amplitude of the MeOH CH_3(ss) peak increases to a maximum value near $\chi = 0.6$. This suggests that the same general behavior is occurring at both interfaces, and coverage–orientation is maximized near $\chi = 0.5$ and then decreases due to density changes and/or the organized adsorption of additional layers of oriented MeOH. We summarize our findings and those of the literature for interfacial MeOH in Table I.

To summarize, the overall interaction strengths of FC and HC monolayers with water and MeOH found different, primarily as measured by changes in the interfacial frequencies of directly interacting solvent molecules. For the FC coatings, the greater lipophobicity of the fluorinated surfaces leads to less interaction between MeOH and the FC monolayer relative to the HC monolayer; this effect is evidenced by the higher frequency of the MeOH CH_3(ss) at the FDS interface. This is consistent with the weaker water–SAM interaction for fluorinated SAMs versus hydrocarbon SAMs, evidenced spectroscopically in a blue-shifting, free-OH oscillator.[16] Having both established these frequency shifts as a measure of interaction strength and examined a neutral polar molecule, the next step is to understand the differences between the adsorption of charged species at FDS and ODS interfaces.

Butylamine HCl. A simple amine salt, $BuNH_3Cl$, was selected for comparative studies at both FC and HC monolayers via VSFS and contact-angle measurements. The use of this molecule allowed us to probe the effects of surface charge on the adsorption of such a highly soluble species and to look for possible specific interactions between $BuNH_3Cl$ and FC or HC monolayers. To study these effects, we used a strategy of isotopically substituted amine chlorides and adsorption at different bulk pH values.

The fused silica substrate on which the ODS and FDS SAMs

TABLE I. Comparison of CH_3OH and H_2O figures of merit at FDS, ODS, and air interfaces. Vibrational frequencies of CH_3OH and H_2O, ΔG° of CH_3OH, and bulk concentration with maximum effective surface density. The free energy of adsorption on FDS is calculated from the MeOH adsorption isotherm.

Figure of merit	FDS	ODS	Air
CH_3OH (location)	2838 $\pm$ 2 cm^{-1}	2831 $\pm$ 4 cm^{-1}	2836 $\pm$ 2 cm^{-1}[a]
Free OH (cm^{-1})	3694 $\pm$ 2 cm^{-1}	3674 $\pm$ 2 cm^{-1}	3704 $\pm$ 2 cm^{-1}[b]
CH_3OH–ΔG°	-1.7 ± 0.1 kcal/mol	-1.6 ± 0.2 kcal/mol [c]	-1.6–2.1 kcal/mol [d]
χCH_3OH at $N_{s,max}$	0.4	0.5	0.5[d]

[a] Datum from Ma and Allen.[73]
[b] Datum from Raymond et al.[80]
[c] Datum from Liu et al.[67]
[d] Datum from Chen et al.[81]

are deposited is known to have a charged surface in aqueous solutions, the charge of which depends on the bulk pH.[82–84] Such a surface charge creates an electrostatic field that orients water molecules in the interfacial region, causing their dipoles to align with the field. This orientation gives rise to the VSFS signal seen in the 3200 cm^{-1} region; we previously showed that both FDS and ODS SAMs exhibit similar charging behaviors, but that these behaviors are modified by the monolayer defect states and likely the substrate to substrate variations of silica plates.[16] To examine the effects of interfacial charge on $BuNH_3Cl$ adsorption, we first look at the aqueous structure at our ODS and FDS surfaces at pH 2 and 5.7. Fused silica is thought to have a net zero charge at pH 2 and be negatively charged at higher pH.[82] These different charge states could well have an effect on the amine adsorption process. To establish the charging behavior at the interface, we first examine the spectra of interfacial water at different bulk pHs by using $BuNH_3Cl$.

Figure 8 shows VSFS spectra of the water–monolayer interface at pH 5.7 with different concentrations of butylammonium chloride. In our previous work, we showed that there is a negative electrostatic field present at both water–FDS and water–ODS interfaces at this bulk pH.[16] This field gives rise to the oriented water signals seen in the 3200 cm^{-1} region of the spectra in Fig. 8. The narrow, isolated feature near 3700 cm^{-1} is from those water molecules straddling the interface that have one OH oscillator pointed into the hydrophobic monolayer and is commonly seen at hydrophobic interfaces.[10,60,61] The principle difference between the water signal being relatively strong in the neat water–FDS spectrum in Fig. 8a and the neat water–ODS spectrum in Fig. 8b, which is relatively weak, was proposed to be the screening of interfacial charge.[16] However, given the variations between individual substrates and coatings, one cannot explicitly assume identical charge in the systems. They might or might not have the same number of accessible SiOH sites for water to interact with once equilibrium is reached, as this will be affected by the detailed surface structure of the silane cross-linkages and the number of defects in the coating. If the substrate charges are the same, then the effective surface charge that is felt at the SAM–solution interface will be different for the two surfaces, with the FDS surface having a stronger field at the chain terminus. If the substrate charge for the SiO_2–FDS system is greater than for the ODS system, due to a greater number or molecular scale defects caused by the shorter, fatter FDS chains, then the field at the solution–FDS interface will be even stronger. Because the $BuNH_3$ ion is positively charged, we expect it will be more attracted to the clear negative electrostatic potential at the FDS–solution interface and have a larger effect on the interfacial water spectra; this is what occurs.

In Fig. 8a, the water signal decreases dramatically with the addition of 1 mM $BuNH_3Cl$, as the interfacial charge from the FDS–water interface is neutralized and screened by the presence of the ions. At 10 mM, signal originating from coordinated water molecules is nearly zero, indicating that there is no net interfacial charge. Increasing the solute concentration to 100 mM results in an increase in the intensity of the coordinated water signal and a reversal of the relative phase of these water modes. This is a clear indication that the interfacial charge has reversed due to the presence of $BuNH_3^+$ ions at the interface. This effect increases with additional $BuNH_3^+$. The same general trends hold true for $BuNH_3Cl$

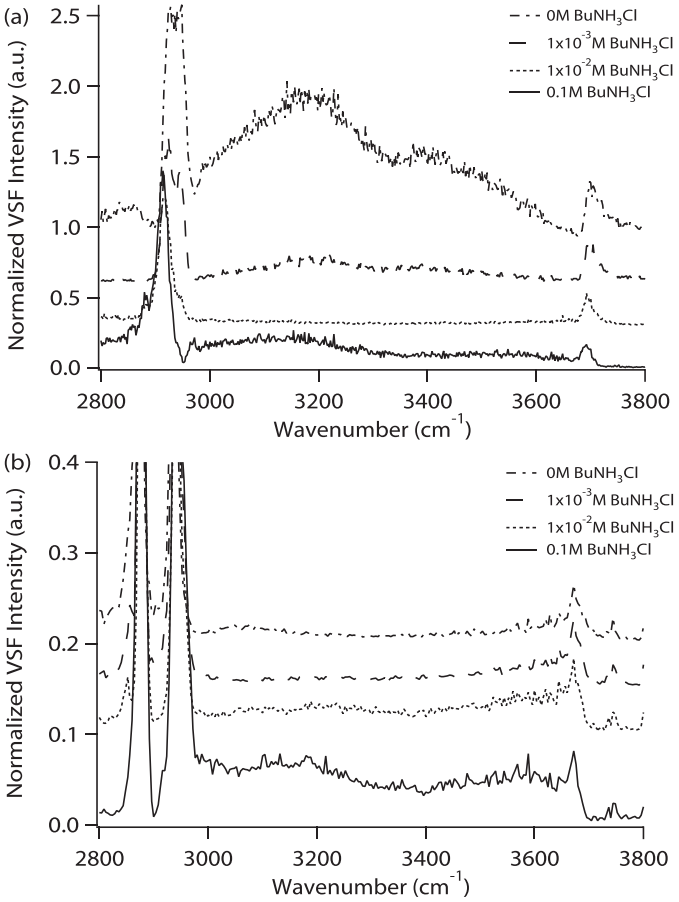

FIG. 8. VSFS spectra of $BuNH_3Cl$ adsorbing onto a (**a**) FDS or (**b**) ODS monolayer in at pH 5.7. The spectra were offset and truncated for clarity.

added to the ODS interface, as seen in Fig. 8b; the addition of the amine salt results in an eventual increase in the intensity of the coordinated water signals in the 3200 cm^{-1} region of the spectrum. Were there no adsorption of $BuNH_3Cl$ to the interface, the charge reversal would not occur, because the ions would merely screen in accordance with the principles of the double-layer model, not unlike what is seen with aqueous NaCl at these interfaces.[16]

At pH 2, the monolayer surface is neutral to slightly positively charged, based on earlier VSFS results.[16] Even with this differently charged starting point, the interfacial water behavior is virtually identical to that of water at pH 5.7 with the addition of $BuNH_3Cl$. Figure 9a shows SSP-polarized VSF spectra of aqueous solutions of d_9–$BuNH_3Cl$ at the FDS surface. With no amine salt present, there is little or no coordinated water signal present; only the CH_2 modes at 2917 and 2954 cm^{-1} and the free OH at 3693 cm^{-1} are present. At 1 mM amine, a small signal originating from coordinated water molecules is present. Increasing the concentration of amine results in further increases in the 3000 to 3600 cm^{-1} region. It is possible that some of this signal arises from NH_3^+, but we are unable to distinguish those contributions from water. By the time the concentration is 100 mM, the signal is much greater. This increase in signal is indicative of interfacial charge reversal.

Comparing the ODS and FDS interface at this pH, we see similar trends in the water behavior. Water-stretching-region spectra of ODS at pH 2 are shown in Fig. 9b. Initially, at pH 2

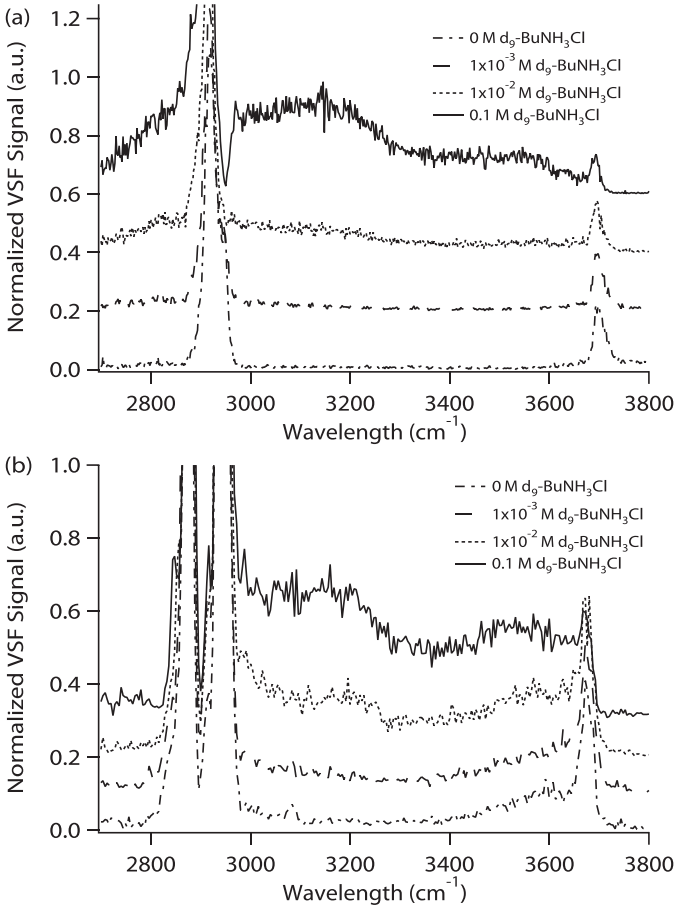

FIG. 9. VSFS spectra of d_9–$BuNH_3Cl$ adsorbing onto a (**a**) FDS or (**b**) ODS monolayer in pH 2 HCl. The spectra were offset and truncated for clarity.

with no amine present, there is no signal present from coordinated water molecules. The spectrum shows the C–H stretches of the ODS monolayer, the free-OH near 3670 cm^{-1} and the small, broad peak due to solvating water molecules near 3600 cm^{-1}.[16] Addition of d_9–$BuNH_3Cl$ to the interface increases the water signal in the 3000 to 3600 cm^{-1} range, as the positively charged adsorbate populates the interface, introducing charge that electrostatically orients water molecules in the interfacial region. Based on this, amine adsorption begins at the same concentration at the pH 2 ODS interface as at FDS.

At both pH 2 and 5.7, adsorption of $BuNH_3Cl$, as measured by changes in the coordinated water region of the spectra, begins at the same concentration, ≈1 mM. Furthermore, adsorption appears to begin at ≈1 mM regardless of the chemical makeup of the SAM, be it hydrocarbon or fluorocarbon. From this set of observations, we can draw two conclusions. First, the amine is preferred to a similar extent over water at both of these interfaces, i.e., the difference in the chemical potential of the ODS–$BuNH_3Cl$–H_2O and ODS–H_2O interfaces is nearly identical to that of the FDS systems. Second, adsorption of $BuNH_3Cl$ occurs regardless of the interfacial charge state, which means adsorption of these molecules is driven by hydrophobic interactions and bulk solubility effects.

To verify these findings from VSFS, we performed contact-angle measurements of $BuNH_3Cl$ on both FDS and ODS at pH 2 and 5.7. These measurements are detailed in the supplemental material available online. There is no change in the contact angles at low concentrations; in fact, the contact angles do not begin to decrease until the $BuNH_3Cl$ concentration is 0.1 M. This supports the observations in our lab that surface tensiometry is less sensitive to interfacial behavior than VSFS. Furthermore, the contact-angle results support the findings that $BuNH_3Cl$ adsorbs identically at both bulk pHs. The calculated free energy of adsorption is the same for FDS at both pH values, −1.9 kcal/mol. This value is slightly smaller than that of ODS, which is calculated to be −2.3 kcal/mol. Finally, the mean molecular areas of the adsorbate at the FDS and ODS interfaces are different, with the area of $BuNH_3Cl$ at FDS being approximately half that at ODS. These results suggest that there are differences in the behavior of $BuNH_3Cl$ at these interfaces at high concentrations.

To gain more detailed insight into the behavior of $BuNH_3Cl$ at these two interfaces, we measured several concentrations of amine chloride with VSFS at both FDS and ODS at pH 2. Our findings show that there is a difference in the adsorbed structure of $BuNH_3Cl$ at these two interfaces due to the differences in interaction strengths between hydrocarbons and fluorocarbons. For simplicity, we began with adsorption at an ODS monolayer by using $BuND_3Cl$–D_2O solutions to remove N–H and O–H stretching contributions from the collected spectra. Attaining a high level of detail regarding adsorption at this surface was not possible in this study because of the overlap of all of the adsorbate vibrational modes with those of ODS. Thus, for this discussion, we limit analysis to 1 M solutions. VSF spectra of this interface with and without $BuND_3Cl$ are shown in both SSP and SPS polarizations in Fig. 10. in the SSP data, shown in Fig. 10a, the 1 M spectrum has much more intensity in the CH_3(ss) near 2870 cm^{-1}. Additionally, in this figure, a small change near 2850 cm^{-1} is evident, which indicates changes in the CH_2(ss) stretching signal with adsorption. SPS spectra in Fig. 10b show a clear increase in intensity of the CH_3(as) vibration in the spectrum with increasing concentration, and a decrease in the intensity below 2900 cm^{-1}.

These changes are not immediately interpretable, because the peaks of the monolayer and the amine have the same frequencies. However, examination of the interface by using fully deuterated d_9–$BuND_3Cl$ at the same concentration found that there were no changes in the ODS spectra. Thus, the differences between the spectra in Fig. 10 are caused by added $BuND_3Cl$, not effects of the adsorbate on monolayer structure. This yields a powerful qualitative observation for this interfacial system—the CH_3 group of the amine is oriented in the same direction as the ODS methyl group. We are able to make this determination, because the increased amplitude of the CH_3(ss) and CH_3(as) vibrational peaks in the spectra indicates that the vibrational resonances of the amine methyl group are in phase with those of the monolayer.

The FDS monolayer, with its simpler CH spectrum, provides an opportunity for a more nuanced examination of amine adsorption. We initially examined the monolayer with D_2O and the fully deuterated d_9–$BuND_3Cl$ at 1 M concentration and found no changes in the intensities of the CH_2; given the proximity of the FDS CH_2 groups to the substrate, these moieties are expected to be unaffected by the addition of amine. VSF spectra, in both SSP and SPS polarizations, of $BuND_3Cl$ at the FDS–D_2O interface are pictured in Fig. 11. At

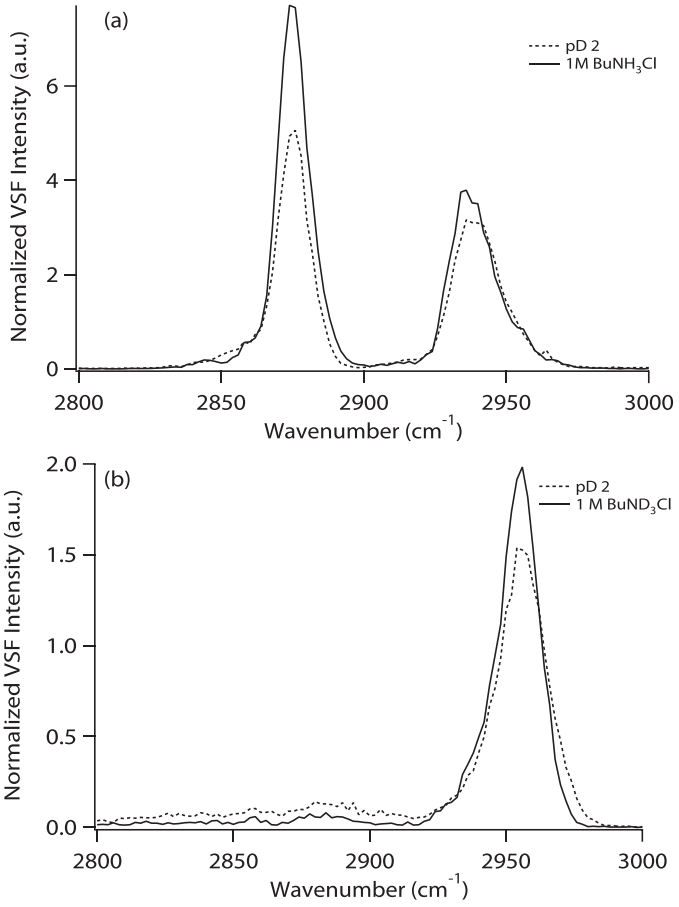

FIG. 10. (**a**) SSP and (**b**) SPS spectra of the C–H stretching region of an ODS monolayer with $BuND_3Cl$ in pD 2 D_2O.

pD 2, the spectrum contains resonances due to the monolayer alone; there is no amine present, and the OD and ND stretching vibrations were shifted out of the spectral window by isotopic substitution. Addition of $BuND_3Cl$ causes major changes in the VSFS data; new peaks appear between 2850 and 2900 cm^{-1}, and the monolayer CH_2 resonances appear to grow thanks to their interferences with modes from the added amine.

We restricted detailed analysis to the region below 2900 cm^{-1}, where two peaks are present. The lower-frequency peak that is the smaller component arises from the CH_2(ss) vibrations of the butyl chain. The fact that this peak is observed could indicate the presence of gauche conformations in the chain, as is known for long-chain molecules[18,45,85] and could be expected for the amine because of weak cooperative interactions between the chains. However, with only three CH_2 groups present in the amine, each one can be expected to have a unique molecular environment, which would both cause slight frequency differences between them and cause their transition dipole moments to not cancel out. This is consistent with the broadness of the measured peak width relative to the CH_3(ss) (11 versus 6 cm^{-1}), and with the results of Chow et al., who found that CH_2 groups in well ordered chains can have different frequencies.[86] For simplicity's sake, we treat this as a single peak centered around 2952 cm^{-1}.

The CH_3(ss) is the largest peak present below 2900 cm^{-1} in Fig. 11a. Spectral fitting analysis places this peak at 2882 ± 1 cm^{-1}, which is blue shifted by ≈10 cm^{-1} from the normal location of an alkyl chain CH(ss) at 2873 cm^{-1}. This frequency

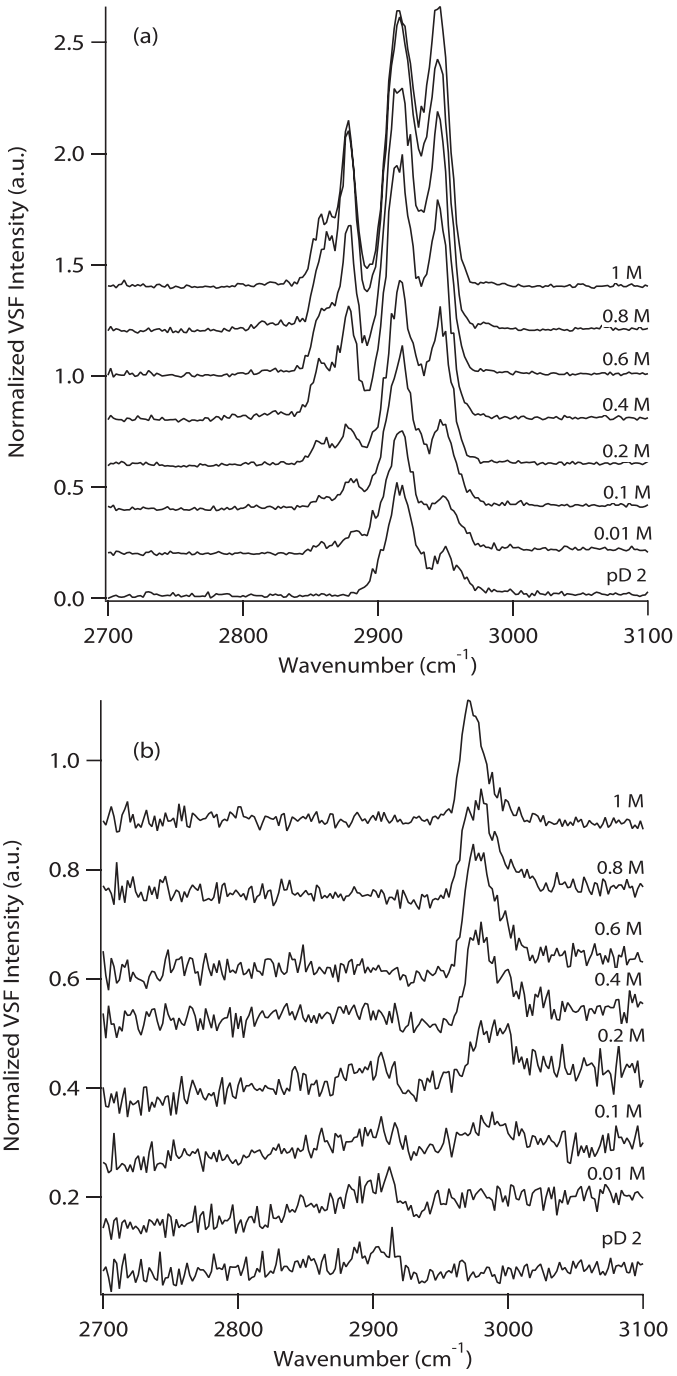

FIG. 11. VSFS spectra of $BuND_3Cl$ on the FDS surface in pD 2 D_2O in (**a**) SSP and (**b**) SPS polarizations. Spectra are offset for clarity.

shift is similar to that seen in the previous section for MeOH at FDS versus ODS (2838 versus 2830 cm^{-1}) and shows that the methyl group of $BuND_3Cl$ is pointed toward the FDS monolayer, directly interacting with it. The presence of this peak and the absence of a distinct peak above 2960 cm^{-1} from a CH_3(as) indicate that the methyl groups are, on average, oriented with their transition dipole moments normal to the interfacial plane. The CH_3(as) transition dipole moment is 180° out of phase with the symmetric stretch and appears in the SPS spectra in Fig. 11b as a sharp resonance at 2968 cm^{-1}. The small feature near 2925 cm^{-1} in the neat pD 2 SPS spectrum

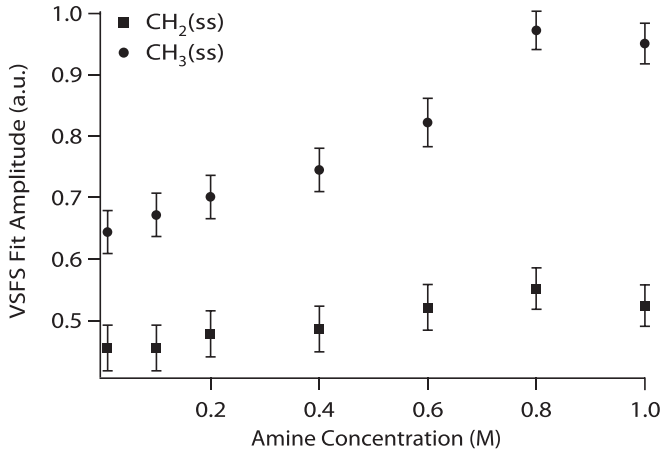

FIG. 12. SSP fit amplitudes of the CH_2(ss) and CH_3(ss) peaks at 2952 and 2882 cm^{-1}, respectively, as a function of $BuND_3Cl$ concentration at pD 2 on FDS.

arises from the CH_2 stretching vibrations of the FDS layer and disappears at higher concentrations due to interference with CH_2 signals from $BuND_3Cl$.

Careful examination of spectra collected between 0.01 M and 1 M reveals some interesting trends. First, the ratio of CH_3(ss)–SSP to CH_3(as)–SPS is nearly constant from 0.6 to 1 M, indicating that the methyl group does not change orientation once this bulk concentration is reached. More information can be gleaned from the CH_2(ss) and CH_3(ss) peaks of the SSP data. As shown in Fig. 12, the amplitudes of both peaks increase with concentration, but at different rates. The amplitude of the CH_3(ss) increases more rapidly than that of the CH_2(ss), indicating that the orientation of the butyl chain changes as it adsorbs to the surface, possibly becoming more ordered. This general behavior has been seen for surfactant adsorption at several interfaces, including hydrophobic ones.[18,19,43,87,88]

Based on these VSFS and contact–angle analyses, a picture of the adsorbate at the two interfaces can be drawn. By using the peak location of the CH_3(ss) and the phase relations between the methyl symmetric and asymmetric stretches, it is clear that the CH_3 group of $BuNH_3Cl$ interacts directly with the FDS layer and juts into the interfacial plane. Based on these results, we suggest that $BuNH_3Cl$ adopts an orientation similar to that in Fig. 13a. In the case of adsorption at ODS, the addition of $BuNH_3Cl$ increases the intensity of the methyl stretching modes, indicating that this group is oriented in the same direction as the monolayer chains. To reconcile this conclusion with the greater molecular area determined from the contact-angle results, the most likely configuration of $BuNH_3Cl$ at the ODS interface is an extended, more lamellar conformation, such as that shown in Fig. 13b. The extended conformation at ODS maximizes the molecular interaction between ODS and the butyl chain, while the more perpendicular orientation at FDS minimizes the FC–HC interactions.

The overall results of this analysis of $BuNH_3Cl$ can be summarized as follows: At pH 2, there is no apparent electrostatic attraction between the SAM–SiO_2 system and the adsorbate. As $BuNH_3Cl$ is added to the solution, its adsorption is first observed in the growth of coordinated water VSFS response near 0.01 M bulk concentration. This is caused by the excess of positively charged adsorbate at the SAM–

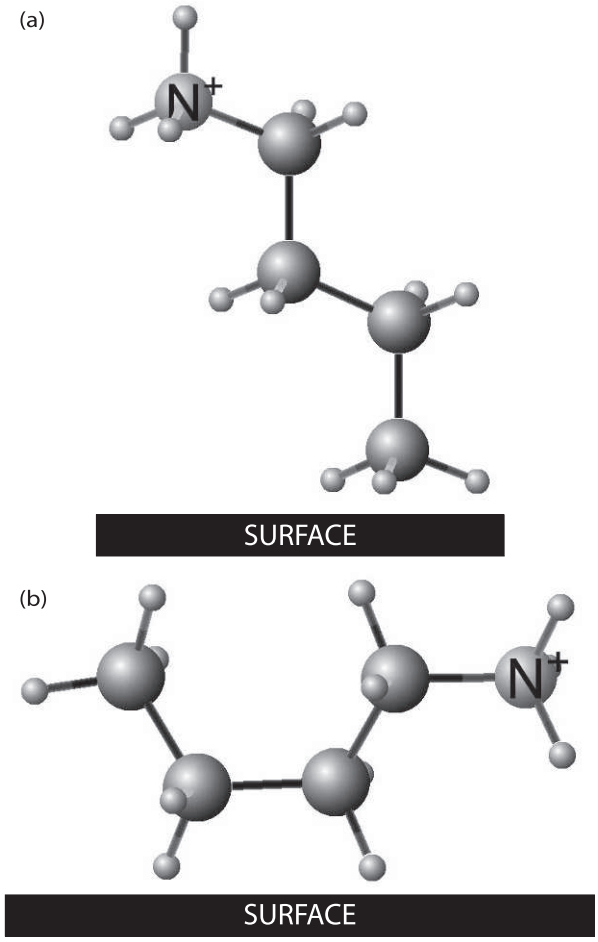

FIG. 13. Two possible confirmations of $BuNH_3Cl$: (**a**) CH–CF interactions minimized at FDS and (**b**) CH–CH interactions maximized at ODS.

water interface. This stage of adsorption occurs before there is any change in the macroscopic measure of adsorption, the water contact angle. The randomly oriented amines begin to adopt a more organized interfacial structure near 0.1 M. This organization is very clear at the FDS interface; with concentrations between 0.1 and 0.6 M, the $BuNH_3Cl$ orientation, as measured by the peak amplitudes, changes to a steady-state value at 0.6 M. At the ODS interface, $BuNH_3Cl$ molecules begin to adopt a net orientation in this same concentration range. It is in this high-concentration region that the contact angle begins to decrease.

The structure of $BuNH_3Cl$ is clearly different at the two interfaces, with the methyl groups adopting different orientations. The thermodynamics of adsorption are energetically less favorable at the FDS interface, and the frequency of the methyl vibrations are blue shifted by $\approx$10 cm^{-1} from their typical frequencies. At ODS, adsorption is slightly more favorable, and the methyl vibrations of $BuNH_3Cl$ are not shifted. This provides experimental verification of the lipophobicity of the fluorocarbon surface and explains the differences in adsorbate conformation. The unfavorable interaction between $BuNH_3Cl$ and FDS results in the minimization of contact area, while this driving force does not exist at the ODS surface. Since the chain–chain interactions of $BuNH_3Cl$ are weak, this unfavorable interaction helps orient them in a more upright conformation. At the ODS surface, this is not the case, and

the molecules are not driven to become well-ordered, but maximize their interactions with the hydrocarbon layer by adopting a more horizontal orientation.

CONCLUSION

To better understand the molecular-scale interactions of adsorbates at fluorocarbon and hydrocarbon surfaces, we analyzed the equilibrium interfacial configurations of two small molecules at FDS and ODS monolayers. The two test molecules are the simplest alcohol and MeOH, and a simple organic salt, butylammonium chloride. These molecules are vibrationally simple and are highly soluble in water, such that they will have minimal van der Waals attractions to each other, allowing us to understand their interfacial behavior in the context of their interactions with the FDS or ODS surface alone.

MeOH adsorbs to the FDS interface at very low concentration due to the great hydrophobicity of the monolayer. As CH_3OH adsorbs, it does so with a constant molecular orientation, displacing interfacial water molecules. This displacement alters the hydrogen-bonding network of interfacial water molecules and thus the coordination of the MeOH OH group. Changes in intermolecular coordination shift the vibrational frequency of the CH_3 group until the coordination number of the interfacial molecules ceases to change near $\chi = 0.5$. On ODS, we see nearly identical behavior. However, due to the favorable interactions between the hydrocarbon SAM and MeOH, MeOH perturbs the monolayer structure slightly and has a different interfacial frequency than at FDS.

For both FC and HC interfaces, $BuNH_3^+$ begins to populate the interface and displace water at relatively low bulk concentrations, behaving as a soluble salt. However, at high concentrations, the amine adsorbs to the monolayer surface and gives the interfacial region a net positive charge, such as a surfactant. At pH 2, this results in electrostatically induced water coordination before there is any ordered adsorption at the interface. Similarly, for both FC and HC SAMs at pH 5.7, $BuNH_3Cl$ first acts mostly as an ion and screens the interfacial charge before reversing it at high concentrations. This charge reversal is not seen with simple salts, such as NaCl and arises from the nonpolar interactions of the carbon chain with the organic coating.

In the high-concentration regime, key differences in the behavior of $BuNH_3Cl$ at FC and HC interfaces become apparent. On the hydrocarbon surface, $BuNH_3Cl$ adopts a relatively horizontal orientation, which maximizes its interactions with the ODS chains. At the fluorinated interface, the terminal methyl group of $BuNH_3Cl$ is oriented toward the fluorocarbon layer, which minimizes the interactions between the adsorbate and the lipophobic monolayer. These observed differences in adsorbate molecular orientation at fluorocarbon and hydrocarbon surfaces show that lipophobic interactions between fluorocarbon and hydrocarbons can affect adsorption processes. These results help explain differences in biomolecule adsorption at fluorocarbon and hydrocarbon surfaces and could lead to different lubricant designs for fluorinated and hydrogenated surfaces.

ACKNOWLEDGMENTS

Thanks are given to Professor Fred Moore at Whitman College for his help in editing this manuscript. The work was supported by the U.S. Department of Energy, Office of Basic Energy Sciences, Division of Materials Sciences and Engineering under award DE-FG02-96ER45557.

SUPPLEMENTAL MATERIAL

Contact-angle analysis used to confirm the conclusions is available in the online version of the journal, at http://www.s-a-s.org.

1. E. Pierstorff, R. Lam, D. Ho. "Nanoscale Architectural Tuning of Parylene Patch Devices to Control Therapeutic Release Rates". Nanotechnology. 2008. 19(44): 445104.
2. K.C. Wood, J.Q. Boedicker, D.M. Lynn, P.T. Hammon. "Tunable Drug Release from Hydrolytically Degradable Layer-By-Layer Thin Films". Langmuir. 2005. 21(4): 1603-1609.
3. S. Takeuchi, D. Ziegler, Y. Yoshida, K. Mabuchi, T. Suzuki. "Parylene Flexible Neural Probes Integrated with Microfluidic Channels". Lab Chip. 2005. 5(5): 519-523.
4. A.B. Fontaine, K. Koelling, S. DosPassos, J. Cearlock, R. Hoffman, D.G. Spigos. "Polymeric Surface Modifications of Tantalum Stents". J. Endovasc. Surg. 1996. 3(3): 276-283.
5. M. Szycher, A. Armini. "Microporous Coating Provides Superior Stent". Membrane Separation Technol. News. 2003. 21(10): 12.
6. R. Maboudian, C. Carraro. "Surface Chemistry and Tribology of MEMS". Annu. Rev. Phys. Chem. 2004. 55: 35-54.
7. R.P. Ambekar, D.B. Bogy, C.S. Bhatia. "Lubricant Depletion and Disk-to-Head Lubricant Transfer at the Head–Disk Interface in Hard Disk Drives". J. Tribol. 2009. 131(3): 1519-1526.
8. R.Z. Lei, A.J. Gellman, C.F. McFadden. "Alkane Contamination Effects on PFPE Lubricant Bonding to a-CH_x Overcoat". Langmuir. 2001. 17(20): 6240-6247.
9. Q. Du, E. Freysz, Y.R. Shen. "Vibrational Spectra of Water Molecules at Quartz–Water Interfaces". Phys. Rev. Lett. 1994. 72(2): 238-241.
10. S. Ye, S. Nihonyanagi, K. Uosaki. "Sum Frequency Generation (SFG) Study of the pH-Dependent Water Structure on a Fused Quartz Surface Modified by an Octadecyltrichlorosilane (OTS) Monolayer". Phys. Chem. Chem. Phys. 2001. 3(16): 3463-3469.
11. V. Ostroverkhov, G.A. Waychunas, Y.R. Shen. "Vibrational Spectra of Water at Water–α-Quartz (0 0 0 1) Interface". Chem. Phys. Lett. 2004. 386(1-3): 144-148.
12. V. Ostroverkhov, G.A. Waychunas, Y.R. Shen. "New Information on Water Interfacial Structure Revealed by Phase-Sensitive Surface Spectroscopy". Phys. Rev. Lett. 2005. 94(4): 046102/1-046102/4.
13. K.C. Jena, D.K. Hore. "Variation of Ionic Strength Reveals The Interfacial Water Structure at a Charged Mineral Surface". J. Phys. Chem. C. 2009. 113(34): 15364-15372.
14. H. Noguchi, M. Hiroshi, T. Tominaga, J.P. Gong, Y. Osada, K. Uosaki. "Interfacial Water Structure at Polymer Gel–Quartz Interfaces Investigated by Sum Frequency Generation Spectroscopy". Phys. Chem. Chem. Phys. 2008. 10(32): 4987-4993.
15. J. Kim, G. Kim, P.S. Cremer. "Investigations of Polyelectrolyte Adsorption at The Solid–Liquid Interface by Sum Frequency Spectroscopy: Evidence for Long-Range Macromolecular Alignment at Highly Charged Quartz–Water Interfaces". J. Am. Chem. Soc. 2002. 124(29): 8751-8756.
16. A.J. Hopkins, C.L. McFearin, G.L. Richmond. "SAMs Under Water: The Impact of Ions on the Behavior of Water at Soft Hydrophobic Surfaces". J. Phys. Chem. C. 2011. 115(22): 11192-11203.
17. R.N. Ward, P.B. Davies, C.D. Bain. "Orientation of Surfactants Adsorbed on a Hydrophobic Surface". J. Phys. Chem. 1993. 97(28): 7141-7143.
18. C.D. Bain, P.B. Davies, R.N. Ward. "In Situ Sum Frequency Spectroscopy of Sodium Dodecyl Sulfate and Dodecanol Co-adsorbed at a Hydrophobic Surface". Langmuir. 1994. 10(7): 2060-2063.
19. R.N. Ward, P.B. Davies, C.D. Bain. "Co-adsorption of Sodium Dodecyl Sulfate and Dodecanol at a Hydrophobic Surface". J. Phys. Chem. B. 1997. 101(9): 1594-1601.
20. R. Windsor, D.J. Neivandt, P.B. Davies. "Adsorption of Sodium Dodecyl Sulfate in the Presence of Poly(ethylenimine) and Sodium Chloride Studied Using Sum Frequency Vibrational Spectroscopy". Langmuir. 2001. 17(23): 7306-7312.
21. M.T.L. Casford, P.B. Davies, D.J. Neivandt. "Study of the Co-adsorption of an Anionic Surfactant and an Uncharged Polymer at the Aqueous Solution–Hydrophobic Surface Interface by Sum Frequency Spectroscopy". Langmuir. 2003. 19(18): 7386-7391.
22. R. Windsor, D.J. Neivandt, P.B. Davies. "Temperature and pH Effects on the Co-adsorption of Sodium Dodecyl Sulfate and Poly(ethylenimine)". Langmuir. 2002. 18(6): 2199-2204.
23. J. Kim, T.S. Koffas, C.C. Lawrence, G.A. Somorjai. "Surface Structural

Characterization of Protein- and Polymer-Modified Polystyrene Microspheres by Infrared–Visible Sum Frequency Generation Vibrational Spectroscopy and Scanning Force Microscopy". Langmuir. 2004. 20(11): 4640-4646.
24. M.T.L. Casford, P.B. Davies, N.J. Neivandt. "Adsorption of Sodium Dodecyl Sulfate at the Hydrophobic Solid–Aqueous Solution Interface in the Presence of Poly(ethylene glycol): Dependence upon Polymer Molecular Weight". Langmuir. 2006. 22(7): 3105-3111.
25. Z. Chen, R. Ward, Y. Tian, F. Malizia, D.H. Gracias, Y.R. Shen, G.A. Somorjai. "Interaction of Fibrinogen with Surfaces of End-Group-Modified Polyurethanes: A Surface-Specific Sum Frequency-Generation Vibrational Spectroscopy Study". J Biomed. Mater. Res. 2002. 62(2): 254-264.
26. J. Kim, G.A. Somorjai. "Molecular Packing of Lysozyme, Fibrinogen, and Bovine Serum Albumin on Hydrophilic and Hydrophobic Surfaces Studied by Infrared-Visible Sum Frequency Generation and Fluorescence Microscopy". J. Am. Chem. Soc. 2003. 125(10): 3150-3158.
27. J. Wang, M.A. Even, X. Chen, A.H. Schmaier, J.H. Waite, Z. Chen. "Detection of Amide I Signals of Interfacial Proteins In Situ Using SFG". J. Am. Chem. Soc. 2003. 125(33): 9914-9915.
28. X. Chen, M.L. Clarke, J. Wang, Z. Chen. "Sum Frequency Generation Vibrational Spectroscopy Studies on Molecular Conformation and Orientation of Biological Molecules at Interfaces". Int. J. Mod. Phys. B. 2005. 19(4): 691-713.
29. X.Y. Chen, J. Wang, J.J. Sniadecki, M.A. Even, Z. Chen. "Probing Alpha-Helical and Beta-Sheet Structures of Peptides at Solid–Liquid Interfaces with SFG". Langmuir. 2005. 21(7): 2662-2664.
30. J. Wang, M.L. Clarke, X. Chen, M.A. Even, W.C. Johnson, Z. Chen. "Molecular Studies on Protein Conformations at Polymer–Liquid Interfaces Using Sum Frequency Generation Vibrational Spectroscopy". Surf. Sci. 2005. 587(1-2): 1-11.
31. D.C. Phillips, R.L. York, O. Mermut, K.R. McCrea, R.S. Ward, G.A. Somorjai. "Side Chain, Chain Length, and Sequence Effects on Amphiphilic Peptide Adsorption at Hydrophobic and Hydrophilic Surfaces Studied by Sum Frequency Generation Vibrational Spectroscopy and Quartz Crystal Microbalance". J. Phys. Chem. C. 2007. 111(1): 255-261.
32. D. Wang, R.D. Oleschuk, J.H. Horton. "Surface Modification of Poly(Dimethylsiloxane) with a Perfluorinated Alkoxysilane For Selectivity Toward Fluorous Tagged Peptides". Langmuir. 2008. 24(3): 1080-1086.
33. A.M. Gaudin, D.W. Fuerstenau. "Streaming Potential Studies—Quartz Flotation with Anionic Collectors". T. Am. I. Min. Met. Eng. 1955. 202: 66-72.
34. D.W. Fuerstenau. "Correlation of Contact Angles, Adsorption Density, Zeta Potentials, and Flotation Rate". T. Am. I. Min. Met. Eng. 1957. 208:(7): 1365-1367.
35. D.W. Fuerstenau. "Streaming Potential Studies on Quartz in Solutions of Ammonium Acetates in Relation to the Formation of Hemi-micelles at the Quartz-Solution Interface". J. Phys. Chem. 1956. 60981-985.
36. M.C. Fuerstenau, K.N. Han. "Metal-Surfactant Precipitation and Adsorption in Froth Flotation". J. Colloid Interface Sci. 2002. 256(1): 175-182.
37. D.W. Fuerstenau, R.H. Jia. "The Adsorption of Alkylpyridinium Chlorides and Their Effect on the Interfacial Behavior of Quartz". Colloids Surf., A. 2004. 250(1-3): 223-231.
38. D.W. Fuerstenau, Pradip "Zeta Potentials in the Flotation of Oxide and Silicate Minerals". Adv. Colloid Interface Sci. 2005. 114-115: 9-26.
39. I.V. Chernyshova, K.H. Rao, A. Vidyadhar, A.V. Shchukarev. "Mechanism of Adsorption of Long-Chain Alkylamines on Silicates: A Spectroscopic Study. 1. Quartz". Langmuir. 2000. 16(21): 8071-8084.
40. I.V. Chernyshova, K.H. Rao, A. Vidyadhar, A.V. Shchukarev. "Mechanism of Adsorption of Long-Chain Alkylamines on Silicates: A Spectroscopic Study. 2. Albite". Langmuir. 2001. 17(3): 775-785.
41. A. Vidyadhar, K.H. Rao, I.V.P. Chernyshova, K.S.E. Forssberg. "Mechanisms of Amine–Quartz Interaction in the Absence and Presence of Alcohols Studied by Spectroscopic Methods". J. Colloid Interface Sci. 2002. 256(1): 59-72.
42. E. Tyrode, M.W. Rutland, C.D. Bain. "Adsorption of CTAB on Hydrophilic Silica Studied by Linear and Nonlinear Optical Spectroscopy". J. Am. Chem. Soc. 2008. 130(51): 17434-17445.
43. X.M. Wang, J. Liu, H. Du, J.D. Miller. "States of Adsorbed Dodecyl Amine and Water at a Silica Surface as Revealed by Vibrational Spectroscopy". Langmuir. 2010. 26(5): 3407-3414.
44. W.T. Liu, L. Zhang, Y. Shen. "Interfacial Layer Structure at Alcohol–Silica Interfaces Probed by Sum Frequency Vibrational Spectroscopy". Chem. Phys. Lett. 2005. 412(1-3): 206-209.
45. P. Guyot-Sionnest, J.H. Hunt, Y.R. Shen. "Sum Frequency Vibrational Spectroscopy of a Langmuir Film: Study of Molecular Orientation of a Two-Dimensional System". Phys. Rev. Lett. 1987. 59(14): 1597-1560.
46. Q. Du, E. Freysz, Y.R. Shen. "Surface Vibrational Spectroscopic Studies of Hydrogen-Bonding and Hydrophobicity". Science. 1994. 264(5160): 826-828.
47. P.B. Miranda, Y.R. Shen. "Liquid Interfaces: A Study by Sum Frequency Vibrational Spectroscopy". J. Phys. Chem. B. 1999. 103(17): 3292-3307.
48. L.F. Scatena, G.L. Richmond. "Orientation, Hydrogen Bonding, and Penetration of Water at the Organic–Water Interface". J. Phys. Chem. B. 2001. 105(45): 11240-11250.
49. V. Buch, T. Tarbuck, G.L. Richmond, H. Groenzin, I. Li, M.J. Shultz. "Sum Frequency Generation Surface Spectra of Ice, Water, and Acid Solution Investigated by an Exciton Model". J. Chem. Phys. 2007. 127(20): 204710.
50. Y.R. Shen. the Principles of Nonlinear Optics. New York: John Wiley, 1984.
51. C.D. Bain. "Sum Frequency Vibrational Spectroscopy of the Solid–Liquid Interface". J. Chem. Soc., Faraday Trans. 1995. 91(9): 1281-96.
52. K.B. Eisenthal. "Liquid Interfaces Probed by Second-Harmonic and Sum Frequency Spectroscopy". Chem. Rev. 1996. 96(4): 1343-1360.
53. G.L. Richmond. "Molecular Bonding and Interactions at Aqueous Surfaces as Probed by Vibrational Sum Frequency Spectroscopy". Chem. Rev. 2002. 102(8): 2693-2724.
54. A.J. Hopkins, C.L. McFearin, G.L. Richmond. "Investigations of the Solid–Aqueous Interface with Vibrational Sum Frequency Spectroscopy". Curr. Opin. Solid State Mater. Sci. 2005. 9(1-2): 19-27.
55. Y.R. Shen, V. Ostroverkhov. "Sum Frequency Vibrational Spectroscopy on Water Interfaces: Polar Orientation of Water Molecules at Interfaces". Chem. Rev. 2006. 106(4): 1140-1154.
56. A.J. Hopkins. In situ analysis of aqueous structure and adsorption at fluorocarbon, hydrocarbon and mineral surfaces. [Ph.D. Dissertation] Eugene, OR: University of Oregon, 2010.
57. C.D. Bain, P.B. Davies, T.H. Ong, R.N. Ward, M.A. Brown. "Quantitative Analysis of Monolayer Composition by Sum Frequency Vibrational Spectroscopy". Langmuir. 1991. 7(8): 1563-1566.
58. S.R. Goates, D.A. Schofield, C.D. Bain. "A Study of Nonionic Surfactants at the Air–Water Interface by Sum Frequency Spectroscopy and Ellipsometry". Langmuir. 1999. 15(4): 1400-1409.
59. R.L. Pizzolatto, Y.J. Yang, L.K. Wolf, M.C. Messmer. "Conformational Aspects of Model Chromatographic Surfaces Studied by Sum Frequency Generation". Anal. Chim. Acta. 1999. 397(1-3): 81-92.
60. E.A. Raymond, G.L. Richmond. "Probing the Molecular Structure and Bonding of the Surface of Aqueous Salt Solutions". J. Phys. Chem. B. 2004. 108(16): 5051-5059.
61. C.L. McFearin, G.L. Richmond. "Understanding How Organic, Solvent Polarity Affects Water Structure and Bonding at Halocarbon–Water Interfaces". J. Mol. Liq. 2007. 136(3): 221-226.
62. D.S. Walker, M. Brown, C.L. McFearin, G.L. Richmond. "Evidence for a Diffuse Interfacial Region at the Dichloroethane–Water Interface". J. Phys. Chem. B. 2004. 108(7): 2111-2114.
63. C.L. McFearin, G.L. Richmond. "The Unique Molecular Behavior of Water at the Chloroform–Water Interface". Appl. Spectrosc. 2010. 64(9): 986-994.
64. L.F. Scatena, M.G. Brown, G.L. Richmond. "Water at Hydrophobic Surfaces: Weak Hydrogen Bonding and Strong Orientation Effects". Science. 2001. 292(5518): 908-912.
65. P. Guyot-Sionnest, R. Superfine, J.H. Hunt, Y.R. Shen. "Vibrational Spectroscopy of a Silane Monolayer at Air Solid and Liquid Solid Interfaces Using Sum Frequency Generation". Chem. Phys. Lett. 1988. 144(1): 1-5.
66. C.S. Tian, Y.R. Shen. "Structure and Charging of Hydrophobic Material–Water Interfaces Studied by Phase-Sensitive Sum Frequency Vibrational Spectroscopy". Proc. Natl. Acad. Sci. U. S. A. 2009. 106(36): 15148-15153.
67. W.T. Liu, L. Zhang, Y.R. Shen. "Interfacial Structures of Methanol: Water Mixtures at a Hydrophobic Interface Probed by Sum Frequency Vibrational Spectroscopy". J. Chem. Phys. 2006. 125(14): 144711/1-144711/6.
68. M. Schwartz, A. Moradi-Araghi, W.H. Koehler. "Fermi Resonance in Aqueous Methanol". J. Mol. Struct. 1980. 63(2): 279-285.
69. M. Schwartz, A. Moradi-Araghi, W.H. Koehler. "Solvent and Temperature Dependence of the Fermi Resonance Parameters in Methanol". J. Mol. Struct. 1982. 81245-252.
70. J.C. Lavalley, N. Sheppard. "Anharmonicity of CH_3 Deformation Vibrations and Fermi Resonance Between Symmetrical CH_3 Stretching Mode and Overtones of CH_3 Deformation Vibrations". Spectrochim. Acta, Part A. 1972. 28(11): 2091-2101.
71. C.J. Gruenloh, G.M. Florio, J.R. Carney, F.C. Hagemeister, T.S. Zwier.

"C–H Stretch Modes as a Probe of H-Bonding in Methanol-Containing Clusters". J. Phys. Chem. A. 1999. 103(4): 496-502.
72. S. Dixit, W.C.K. Poon, J. Crain. "Hydration of Methanol in Aqueous Solutions: A Raman Spectroscopic Study". J. Phys. Condens. Matter. 2000. 12(21): L323-L328.
73. G. Ma, H.C. Allen. "Surface Studies of Aqueous Methanol Solutions by Vibrational Broad Bandwidth Sum Frequency Generation Spectroscopy". J. Phys. Chem. B. 2003. 107(26): 6343-6349.
74. C.Y. Chen, M.L. Clarke, J. Wang, Z. Chen. "Comparison of Surface Structures of Poly(ethyl methacrylate) and Poly(ethyl acrylate) in Different Chemical Environments". Phys. Chem. Chem. Phys. 2005. 7(11): 2357-2363.
75. U. Buck, F. Huisken. "Infrared Spectroscopy of Size-Selected Water and Methanol Clusters". Chem. Rev. 2000. 100(11): 3863-3890.
76. L. Gonzalez, O. Mo, M. Yanez. "High-Level Ab Initio and Density Functional Theory Studies on Methanol–Water Dimers and Cyclic Methanol$(Water)_2$ Trimer". J. Chem. Phys. 1998. 109(1): 139-150.
77. F. Huisken, S. Mohammad-Pooran, O. Werhahn. "Vibrational Spectroscopy of Single Methanol Molecules Attached to Liquid Water Clusters". Chem. Phys. 1998. 239(1-3): 11-22.
78. R.N. Ward, D.C. Duffy, P.B. Davies, C.D. Bain. "Sum Frequency Spectroscopy of Surfactants Adsorbed at a Flat Hydrophobic Surface". J. Phys. Chem. 1994. 98(34): 8536-8542.
79. Y. Liu, L.K. Wolf, M.C. Messmer. "A Study of Alkyl Chain Conformational Changes in Self-assembled *N*-Octadecyltrichlorosilane Monolayers on Fused Silica Surfaces". Langmuir. 2001. 17(14): 4329-4335.
80. E.A. Raymond, T.L. Tarbuck, G.L. Richmond. "Isotopic Dilution Studies of the Vapor–Water Interface as Investigated by Vibrational Sum Frequency Spectroscopy". J. Phys. Chem. B. 2002. 106(11): 2817-2820.
81. H. Chen, W. Gan, R. Lu, Y. Guo, H.F. Wang. "Determination of Structure and Energetics for Gibbs Surface Adsorption Layers of Binary Liquid Mixture. 2. Methanol + Water". J. Phys. Chem. B. 2005. 109(16): 8064-8075.
82. S. Ong, X. Zhao, K.B. Eisenthal. "Polarization of Water Molecules at a Charged Interface: Second Harmonic Studies of the Silica–Water Interface". Chem. Phys. Lett. 1992. 191(3-4): 327-335.
83. P.M. Dove, J.D. Rimstidt. "Silica–Water Interactions". In: P.J. Heany, C.T. Prewitt, G.V. Gibbs, editors. Silica: Physical Behavior, Geochemistry, and Materials Applications. Washington, D.C: Mineralogical Society of America, 1994. Pp. 259.
84. J.L. Daschbach, P.R. Fischer, D.E. Gragson, D. Demarest, G.L. Richmond. "Observation of the Potential-Dependent 2nd-Harmonic Response From the Si^{111}–Electrolyte and Si^{111}–SiO_2–Electrolyte Interfacial Regions". J. Phys. Chem. 1995. 99(10): 3240-3250.
85. J.C. Conboy, M.C. Messmer, G.L. Richmond. "Dependence of Alkyl Chain Conformation of Simple Ionic Surfactants on Head Group Functionality as Studied by Vibrational Sum Frequency Spectroscopy". J. Phys. Chem. B. 1997. 101(34): 6724-6733.
86. B.C. Chow, T.T. Ehler, T.E. Furtak. "High-Resolution Sum Frequency Generation from Alkylsiloxane Monolayers". Appl. Phys. B: Lasers Opt. 2002. 74(4-5): 395-399.
87. K.A. Becraft, F.G. Moore, G.L. Richmond. "Charge Reversal Behavior at the CaF_2–H_2O–SDS Interface as Studied by Vibrational Sum Frequency Spectroscopy". J. Phys. Chem. B. 2003. 107(16): 3675-3678.
88. K.A. Becraft, G.L. Richmond. "Surfactant Adsorption at the Salt–Water Interface: Comparing the Conformation and Interfacial Water Structure for Selected Surfactants". J. Phys. Chem. B. 2005. 109(11): 5108-5117.